MULTIMODAL PLATFORM FOR RAMAN AND NONLINEAR OPTICAL MICROSCOPY AND MICROSPECTROSCOPY FOR CONDENSED MATTER STUDIES

In 2015, the activities of the Sector of Raman Spectroscopy (Centre "Nanobiophotonics") were focused on the further development and enlarging of the spectral and microscopic possibilities of the optical platform "CARS" microscope. This was done with the aim to implement the state of the art optical options for highly spectrally selective imaging and high sensitivity enhanced Raman spectroscopy:

- Polarized Coherent antiStokes Raman Scattering (P-CARS)
- Surface Enhanced Raman Scattering (SERS)
- Raman scattering using laser excitation at 532nm

All three of these options were successfully elaborated and established at the "CARS" microscope. Afterwards, the research activities were carried out on the following tasks: highly selective spectral imaging of membrane proteins; first tests of SERS with various biomolecules; photo- and up-conversion luminescence of oxyfluoride nano-glass-ceramics doped with Er^{3+}, Eu^{3+}, Tm^{3+}, and Yb^{3+}. Some other research activities for JINR labs and Member States were implemented in the frame of the "friendly user facility" as well.

1. The upgraded "CARS" microscope

Figure 1 shows the upgraded schematic of the multimodal optical platform for performing Raman, P-CARS, SERS spectroscopy and microscopy. We exploit parallel orientations of linear polarizations of the input Stokes and pump beams. Both excitation picosecond pulse trains are made coincident in time and in space utilizing an optical delay line and a series of dichroic mirrors. For CARS microscopy a water-immersion objective lens with a high numerical aperture (NA=1.2, UPLANAPO-60x, Olympus) was exploit to focus the beams tightly.

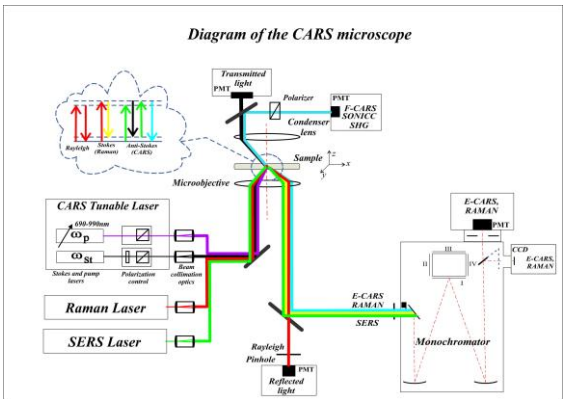

Fig. 1. Diagram of the upgraded multimodal optical platform: "CARS" microscope

Using this optical platform, a sample can be imaged by utilizing vibration frequencies in the spectral range of (1000−3580) cm^{-1}, which covers all most important vibrational modes of bio-molecules. Five detection channels allow two forward- and three backward- propagated signals to be recorded. The polarization control is adjustable with a half-wave plate in the Stokes beam. Along with the CARS signals, the system allows detection of spontaneous Raman, luminescence, including up-conversion luminescence, second and sum frequency generation signals and transmission mode as well.

1. SCIENTIFIC RESEARCH

In 2015 we also incorporate into the our optical system a diode-pumped green laser at 532nm with an adjustable output power of up to 20 mW and more than 50 meters coherence length (model SLM-417-20).

2. Scientific results

2.1 P-CARS imaging of membrane protein crystals

During the reporting period in cooperation with the Institute for the Physics of Complex Systems (Germany), the Institute of Structural Biology (France), Moscow Institute of Physics and Technology, and Orbeli Institute of Physiology (Armenia), research activities on membrane protein (MP) structural studies using nonlinear optical microscopy were initiated. For the first time CARS images of MP crystals with submicron resolution and high contrast were obtained. As a first step in this direction, we performed the studies with bacteriorhodopsin crystals. The C=C retinal chromophore vibrational stretch at 1529 cm-1 is chosen from the Raman spectrum of BR crystals for CARS microscopy imaging.

Figure 2 compares Raman and CARS images of a sizable BR crystal. An optical microscopy image of this crystal is shown in the figure as well (**Fig. 2a**). A Raman intensity map of the C=C stretching vibrations of the retinal chromophore in bacteriorhodopsin is shown in **Fig.2b**. Any of the small sized features is not observed in the Raman image. The analytical capabilities of the spontaneous Raman scattering microscopy are significantly limited by the difficulty in acquiring contrast image with low signals.

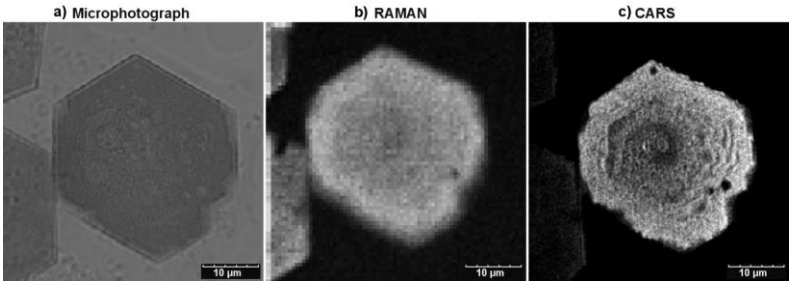

Fig. 2. *a) Microphotograph, b) Raman (λ_{ex}=785nm) and c) P-CARS (λ_p= 915.5nm, λ_{St}=1064nm), images at vibration 1529 cm-1 of bacteriorhodopsin crystal. Scan area – 48x48μ*

The CARS image is much more stronger than the spontaneous Raman signal, allowing very fast imaging acquisition of ~3s with good signal-to-noise ratio. The high spatial resolution of CARS permits visualization of detailed structures in BR crystals. Also, there were obtained P-CARS images of small crystals with submicron resolution.

A few of BR crystals consists of two roughly equal sized parts because of twinning. Twinning is one of the most common crystal-growth defects in protein crystallography. **Figure 3** demonstrated a high quality 3D-imaging of twin BR crystals.

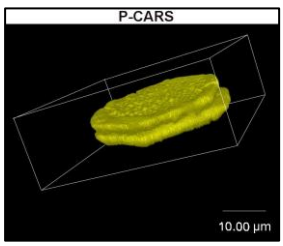

Fig. 3. *P-CARS 3D-image of twin BR crystal*

2.2 Surface Enhanced Raman Scattering (SERS): first experiments

In cooperation with partners from the Republic of Belarus (BSUIR and Scientific-Practical Materials Research Centre of NAS) the spectra of spontaneous Raman scattering and SERS for rhodamine 6G dye (R6G) and protein lysozyme were obtained using a substrate based on porous crystalline silicon. For excitation of the Raman scattering was used either He-Ne laser (632.8 nm) or diode-pump laser with a wavelength of 532nm. The power of the exciting laser exposure is selected experimentally to achieve maximal SERS - effect. The accumulation time of Raman spectrum is varied from 0.5 to 10 seconds.

In 2015 the main research directions goals on SERS were the following:

- definition of the concentration sensitivity limit on the SERS active substrates based on silver/porous silicon (Ag / PS);
- definition of the maximum enhancement factor (EF) on the SERS active substrates based on plasmonic structures Si/SiO_2/(Ag).

2.2.1. SERS - active structures on the basis of silver / porous silicon (Ag/PS) composition

Spontaneous Raman spectrum of lysozyme was obtained at a dilution of its concentration up to 10^{-3} M (control). For obtaining SERS effect was used concentration for 10^4 and 10^6 less than the control: 10^{-7} and 10^{-9} M solution of lysozyme. The power of the exciting laser (632.8 nm) was 250 μW.
Fig. 4 demonstrates enhance Raman signals from lysozyme in SERS option using substrates on the basis of silver/porous silicon (Ag/PS).

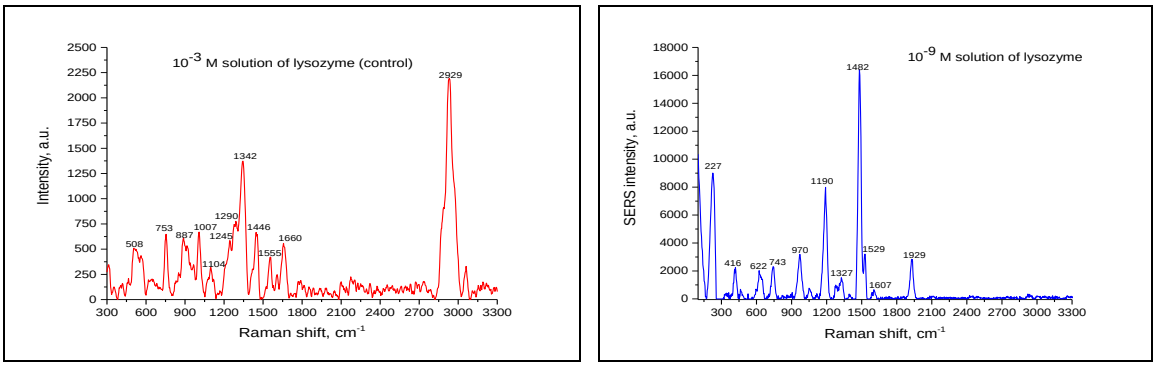

Fig.4. *On the left: Raman spectrum of 10^{-3}M solution of lysozyme (control), on the right: SERS spectrum of 10^{-7}M solution of lysozyme*

SERS allows to identify molecules of lysozyme at the concentration of 10^{-9}M. It appears that the laser power of 250 μW was enough for this enhancement. In 2016 these activities would be proceeded.

2.2.2. Plasmonic structures of Si/SiO2/(Ag)

The second type of substrates exploited in our SERS studies were so-called plasmonic structures of Si/SiO_2(Ag) composition, produced by ion-track technology. Monocrystalline silicon plates served as a surface to develop Si/SiO_2 structures. Substrates of Si/SiO2 were exposed to the Au ions at the energy of 350 MeV. Irradiation was carried out at the normal incidence angle, leading to a random distribution of parallel oriented ion tracks in a layer of SiO_2. Plasmonic structures of Si/SiO_2(Ag) differed from each other by the time of etching in hydrofluoric acid HF (10 - 35 min), which affects the

pore diameter formed in silicon oxide. The pore diameter in turn causes the dendritic morphology of silver nanoparticles when treated with a 0.02 M solution of $AgNO_3$. The obtained results are shown in **Fig. 5.**

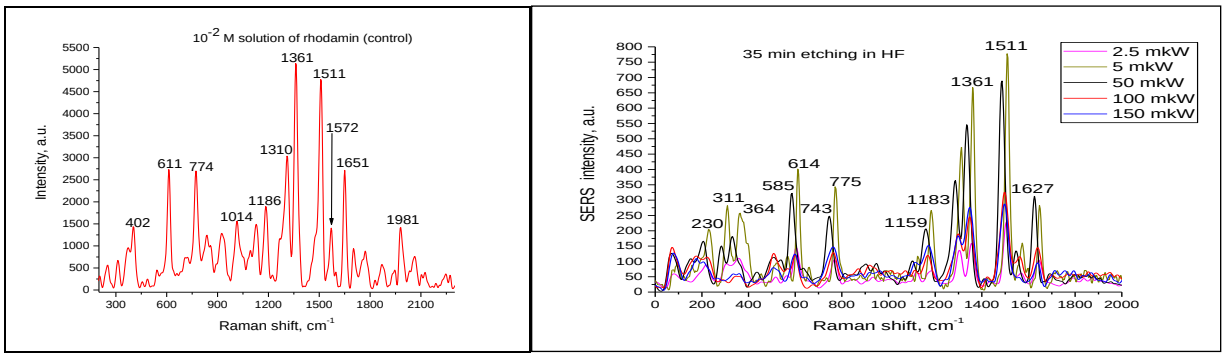

Fig.5. *On the left: Raman spectrum of 10-2M solution of R6G (control); on the right: SERS spectrum of 10-6 M solution of R6G on plasmonic structures of Si/SiO2/(Ag), etching time 35 min*

The results indicate that the best plasmon structures are the substrates with an etching time of 35 minutes, resulting in the SERS enhancement factor of as high as 10^7-10^8 (**Fig. 5, right**). Wherein, the optimal laser power is of 5 μW.

The results obtained in 2015 on SERS studies we consider as very optimistic, thus they can be serve as a good basis for the further research activities in the Sector of Raman spectroscopy, LNP.

2.2 Photo- and up-conversion luminescence (UCL) of oxyfluoride nanoglassceramics doped with rare earth elements (REE)

In 2015, an international collaboration was established with the Institute of Solid State Physics of University of Latvia, Riga, with the Belarusian State Technological University, Minsk, and the Institute of Solid State Physics and Semiconductors, Minsk. The structural and spectral characteristics of oxyfluoride glasses co-doped by europium and ytterbium ions with different molar concentrations.

Structural studies.

The X-ray diffraction analysis (XRD) of precursors and heat-treated samples was done to identify the nanocrystalline phase of lead fluoride. The presence of diffraction peaks in the heat-treated samples indicates the formation of nanocrystalline phase, corresponding to the cubic crystal lattice of PbF_2 nanocrystals. The average size of the nanocrystals ~6,5nm was calculated using the Debye-Scherrer's equation.

Also, transmission electron microscope (TEM) «FEI Tecnai» was exploited to visualize the nanocrystalline phase (**Fig.6**.).

As it is seen from the figure, the PbF_2 nanocrystals are spherical in shape and have relatively small variations in diameter. However, the size dispersion is pronounced to be bimodal: there is a fraction of ~15nm size and a fraction of ~(2-5)nm.

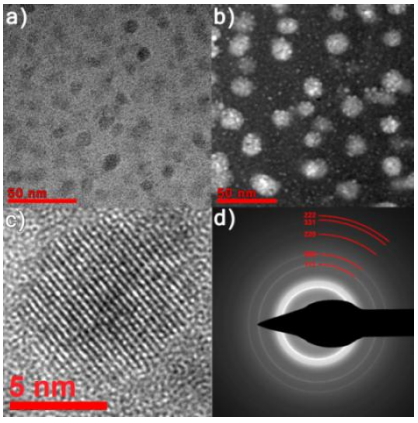

Fig. 6. *TEM images of the heat-treated samples: a) bright-field image, b) dark-field image, c) the enlarged image of nanocrystals, d) electron diffraction pattern of nanocrystal.*

Fig. 6(c, d) shows that nanocrystals have a face-centered cubic lattice crystal, typical for β-PbF_2.

Luminescent characteristics

Photoluminescence spectra of precursor and heat-treated samples were measured under the laser excitations of 325, 405, 456nm, and a xenon lamp at the wavelength of 440nm (**Fig.7**). At the all excitation wavelengths a pronounced red photon emission was observed, typical for *4f-4f* transition of Eu^{3+}.

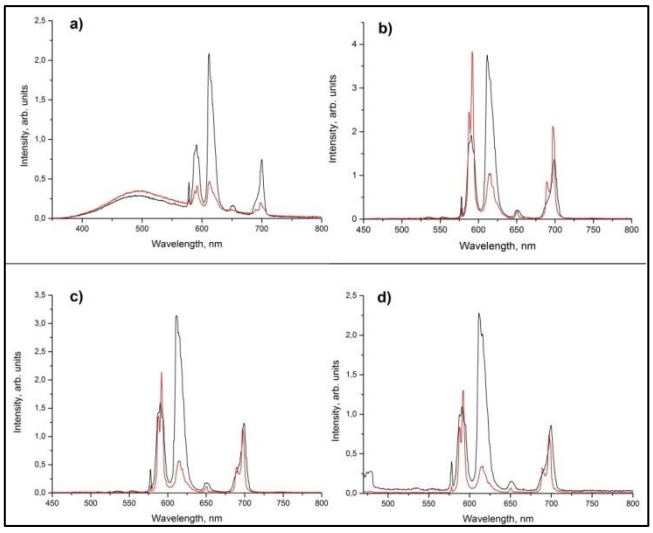

Fig.7. *Photoluminescence spectra at different excitations: a) 325nm b) 405nm c) 440nm d) 457nm*

The spectra of up-conversion luminescence of the precursor and heat-treatment samples were detected at the «CARS» microscope using laser excitation at 976nm corresponding to the maximal value of absorption coefficient of ion Yb^{3+} (**Fig.8**).

As can be seen from **Fig. 5**, in addition to the luminescence bands typical for the europium ions, additional bands are observed at 510, 525, and 550 nm, related, with a high probability, to the erbium ions in the sample as an impurity. Subsequently conducted energy dispersive analysis (EDS) confirmed this assumption. It should be also noted the increase of the erbium peaks in heat-treated samples are due to the inter-ion interaction processes described in details in our previous studies.

1. SCIENTIFIC RESEARCH

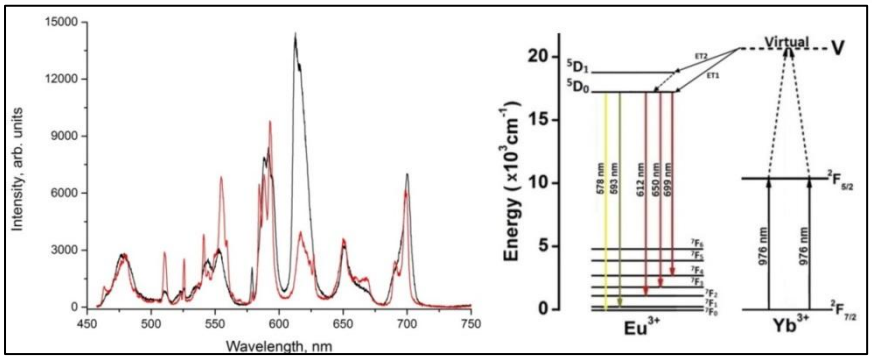

Fig.8. *UCL spectra of precursor and heat-treated sample, excitation 976nm. On right – energy transition diagram for Eu^{3+} ion.*

Presently, the above mentioned results on photo- and UC luminescence are being in preparation for publication in a peer-reviewed journal in this field.

REFERENCES

[1] A. Zumbusch, G.R. Holtom, and X.S. Xie, "Three-Dimensional Vibrational Imaging by Coherent Anti-Stokes Raman Scattering," Phys. Rev. Lett. **82,** 4142-4145 (1999).

[2] J.-X. Cheng, Y. K. Jia, G. Zheng, X.S. Xie, "Laser-Scanning Coherent Anti-Stokes Raman Scattering Microscopy and Applications to Cell Biology", Biophysical Journal **83,** 502-509 (2002).

[3] Andreas Volkmer, "Vibrational imaging and microspectroscopies based on coherent anti-Stokes Raman scattering microscopy", J. Phys. D: Appl. Phys. **38,** R59–R81 (2005).

[4] D.J. Kissick, D. Wanapun, G.J. Simpson, "Second-Order Nonlinear Optical Imaging of Chiral Crystals", Annu. Rev. Anal. Chem. **4,** 419–437 (2011).

[5] Ji-Xin Cheng, Lewis D. Book, and X. Sunnie Xie, "Polarization coherent anti-Stokes Raman scattering microscopy", Opt. Letters, **26**, 1341-1343 (2001).

[6] A. Barhoumi, D. Zhang, F. Tam, N.J. Halas, "Surface-enhanced raman spectroscopy of DNA", J. AM. CHEM. SOC, **130**, 5523-5529, (2008).

[7] T.-W. Koo, S. Chan, A. A. Berlin, "Single-molecule detection of biomolecules by surface-enhanced coherent anti-Stokes Raman scattering", Optics letters, **30 (9)**, 1024-1026, (2005).

[8] J.B. Jackson, S.L. Westcott, L.R. Hirsch, J.L. West, N.J. Halas, "Controlling the surface enhanced Raman", Applied Phys. Lett., **82 (2)**, 257-259, (2001).

[9] G.M. Arzumanyan, V. Vartic, et all "CARS microscope: "Possibilities, the first results, problems and prospects", Communication of JINR, P13-2013-108, Dubna, (2013).

[10] G. Arzumanyan, V.Vartic, A. Kuklin, D. Soloviov, G. Rachkovskaya, et al. "Upconversion Luminescence of Er3+ and Co-Doped Er3+/Yb3+ Novel Transperent Oxyfluoride Glasses and Glass Ceramics: Spectral and Structural Properties" Journal of Physical Science and Application 4, 150-158 (2014).

[11] J. Zhou, Q. Liu, W. Feng, Y. Sun, F. Li "Upconversion Luminescent Materials: Advances and Applications" Chem. Rev., 115(1), 395-465 (2015).

[12] Y.Dwivedi, S.C. Zilio, "Infrared cascade and cooperative multicolor upconversion emission in $Y_8V_2O_{17}$:Eu:Yb nanophosphors" Optical Express, 21, 4717-4177, (2013).